

Figure 3.1 shows the spacecraft above the west limb of the Sun, keeping it above the east limb is also an option if desired for space-weather applications. Similarly, for $n = 3$, the mirror image of that shown in Figure 3.1 is also possible. It can be seen from Table 3.1 and from the bottom row in Figure 3.1 that, because of the resonance conditions, the spacecraft is always in good view from Earth, with no close conjunctions or occultations.

The fourth row in Table 3.1 contains an estimate of the extremely large change in velocity, Δv , that must be imparted to the spacecraft to place it in polar orbit. What are the options for achieving such polar orbits?

- Chemical Propulsion with Planetary Gravity Assists:
 - Jupiter gravity assist: Such orbits have aphelion distances near Jupiter. The possibilities are limited to circular orbits at a great distance from the Sun (~ 5 AU) or a Ulysses-type eccentric orbit with perihelion as close to the Sun as one wishes. The current plans for the Solar Probe are based on such a trajectory. The Jupiter flyby option cannot meet the requirements for circular orbits at ≤ 1 AU.
 - Earth and/or Venus gravity assists. It is possible to obtain a 1-AU circular trajectory with an inclination of 30° to the ecliptic in 4.8 years with two Venus and two Earth gravity assists. Further Earth flybys could slowly crank the orbit to still higher inclinations, but the total mission time to reach 90° inclination is unrealistically long.
- Solar Electric Propulsion (SEP). A 5 kW SEP system can deliver a 230 kg payload to a 1 AU circular orbit with a 47° (heliographic) inclination in about 6.5 years using a Delta II/7925 launch vehicle. (This ignores the degradation of the solar arrays over the course of the mission.) The time to a truly polar orbit is again excessive and/or a larger, more expensive SEP system and launch vehicle would be required.
- Solar Sail. Solar sail propulsion was studied in the 1970s for possible use in a mission to rendezvous with Comet Halley. The sail was huge — ~ 830 m on a side. Recent technological developments of smaller and lighter spacecraft subsystems and instruments make the solar-sail option more attractive than it was 20 years ago. The bottom row in Table 3.1 gives flight times for achieving circular orbits with 90° inclination using a solar sail 200 m on a side. Although the cruise times to the final orbits are still rather long, solar sail propulsion appears to be the only practical means by which the mission objectives can be achieved.

With solar sail, the flight time depends on the mass to be delivered to the final orbit as well as on the mass and reflective area of the sail. The figure of merit for the sail system mass (sail + its support structure + its deployment and control mechanisms) is the effective density or sail loading, given in g/m^2 . For a given sail loading, the trades between net or delivered mass, the acceleration, sail size, and total launched mass (the “sailcraft” mass) are shown in Figures 3.2 and 3.3 for a sail loading of 6 g/m^2 .

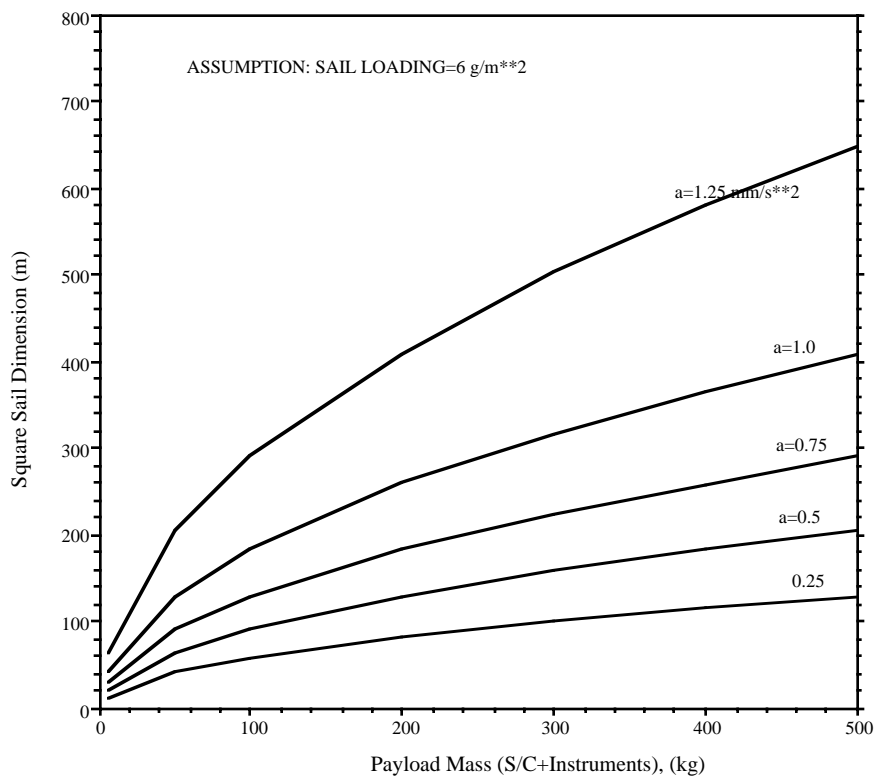
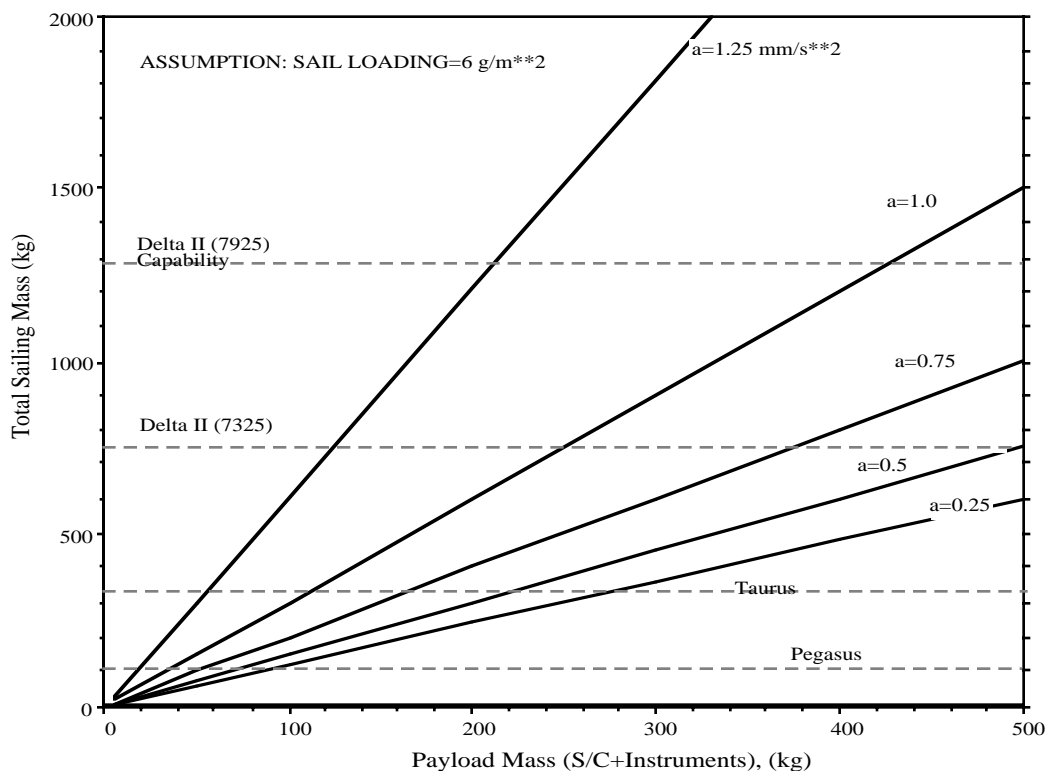


Figure 3.2 (above) Sail size versus net spacecraft mass as a function of acceleration at 1 AU. Each curve corresponds to a different value of acceleration, a , which is given in units of mm/s^2 .

Figure 3.3 (below) Total launched mass vs delivered spacecraft mass as a function of acceleration at 1 AU.



The maximum allowable sailcraft mass depends on the launch vehicle, with limits of approximately 420, 660, 1300, and 2700 kg for the Taurus XL/Star 37FM, the Delta II/7325, the Delta II/7925, and the Atlas IIAS, respectively.

Only the $n = 3$ option is considered for the remainder of this study. That option was chosen because of the advantages accruing from being closer to the Sun than 1 AU (e.g., smaller optical instruments; fewer stream interactions between the Sun and point of in situ measurements of the solar wind; better capability to study the impulsive component of solar energetic particles; better resolution for separating latitudinal versus temporal effects) while keeping the spacecraft within 30° of the solar limbs for a substantial fraction of the time. Plots of some of the trajectory parameters for the $n = 3$ case are presented in Appendix B.

Table 3.2 presents flight times to an $n = 3$ polar orbit for several choices of sail size, sail loading, and launch vehicle. The figures are based on the 230 kg delivered mass (spacecraft + instruments) consistent with the results of the technical feasibility study described in Section VII.

TABLE 3.2. FLIGHT TIMES FOR DELIVERY OF A 230-KG SPACECRAFT TO A CIRCULAR POLAR ORBIT AT 0.48 AU

Sail Size m on a side	Sail Loading g/m²	Sailcraft Mass kg	Launch Vehicle	Time to Orbit yrs
150 (1)	6.8 (1)	382	Taurus	5.15
158 (2)	6.0 (2)	380	Taurus	4.59
200	7.0	510	Delta II/7326	3.88
200 (3)	6.8 (3)	502	Delta II/7326	3.76
200	6.0	470	Delta II/7326	3.52
200	5.8	462	Delta II/7326	3.48

(1) DLR sail design

(2) Assumptions used for Team X study described in Section VII

(3) Assumptions used for Table 3.1

More information on the solar sail is given in Section VI.

IV. Science Instruments

A strawman payload has been developed to address the objectives discussed in Section II in order to provide the instrument requirements as input to the technical feasibility study described in Section VII. It is envisioned that the final set of instruments for this mission would be competitively selected, so some of the detailed requirements will certainly differ from those presented here. It is nonetheless useful to determine the broad scope of what is feasible with current or planned technology and within the limits assumed for this mission. In the current political environment, low cost and short mission duration are considered to be highly desirable attributes. For SPSM, these parameters translate into low mass and constraints on the amount of data returned.

A. Coronagraph

The highest priority instrument is a coronagraph. Such an instrument was selected for viewing the Sun from above its poles on the canceled US spacecraft component of the Ulysses mission. Many important scientific discoveries have come from the data acquired by coronagraphs on Skylab, P78-1, the Solar Maximum Mission (SMM), Spartan 201, and SOHO. The unique views from above the poles achievable with SPSM will allow extension of the earlier observations into the third dimension.

Coronal images tend to have relatively low rms variation at spatial frequencies below 3/arcsec. SMM and Skylab images indicate that most of the structures visible in streamers and mass ejections are adequately visualized with a scale of 20 arcsec/pixel. The SOHO-C3 images of CMEs have spatial resolution which is about 1/3 of this, and that device is satisfactory for visualization of the major large scale structures of the corona.

Two approaches to coronagraph design have been used in the past. The first is to visualize the solar corona with an externally occulted telescope set to view the coronal structures from an inner limit set by the smallest occulting disk tolerable to a limit at the outside set by the number of detector pixels and the image scale. Innovations in the collection and suppression of instrumental scattered light have pushed the inner limit of extant coronagraphs to about 1.25 solar radii as measured from the center of the Sun. The second approach is to set an outer limit of the field of view based on flux or geometry considerations and then to set the lower limit of the field of view so that the brightness of the inner corona does not over-expose the detector for exposure times long enough to stimulate pixels which view the far-field corona. Large pixel (large well) CCD imagers and large dynamic range analog-to-digital converters are vital to the success of the second approach. Both approaches have been successfully used to view the corona from 1 AU.

For the present strawman payload, the coronagraph is assumed to have a 10-solar-diameter field of view with an inner limit set by an external occulter of 1.25 solar radii. For a square detector with 1024 pixels per side, the scale would be ~20 arcsec/pixel or a resolution (Nyquist frequency) of 2/3 cycle/arcmin. The optical properties are summarized in Table 4.1.

TABLE 4.1. OPTICAL PROPERTIES OF STRAWMAN CORONAGRAPH

Field of view	1.25 to 10 solar radii
Pixel scale	20 arcsec/pixel
Spatial resolution	40 arcsec; 14,000 km from 0.48 AU
Number of pixels/image	8.2×10^5 (10-diameter circular field of view)
Intensity resolution	14 bits
Bandpass	Single color (500 Å optical bandwidth)
Images/observation	3; 0° and $\pm 60^\circ$ orientation of linear polarization

The strawman coronagraph is based on an externally occulted design. The first objective lens would have a diameter of ~1.0-1.5 cm and could be simpler than the design used in the

Spartan coronagraph. In order to assist in the separation of the K corona (reflection of sunlight from electrons) from the F corona (reflection from dust), each picture is acquired in three different polarizations. Manipulation of the three images yields maps of brightness B , the polarization p , and the product pB . Because the column measurements of p and B have different kernels, measuring p and B separately gives information on where the different signals come from along the line of sight. The polarizers and some filters could be mounted on motor-driven filter wheels, a design that worked well on the Spartan 201 mission. An alternative, mass-saving possibility to be explored is to lay down the polarizers directly on the CCD chip with every third pixel having the same polarization; then only a single image would be required per observation.

The signals from orthogonal strings of diodes in the coronagraph focal plane can be used as the fine sun sensing element of the attitude control system.

Power exists over a wide range of frequencies in the solar corona. Natural time scales are set either by physical processes (velocity and acceleration) or by the lifetimes of structures. During periods intermediate between solar maximum and minimum, coronal streamers last between one and three solar rotations. Large scale features of the chromosphere have typical lifetimes between one day and one-half rotation. Velocities of eruptive prominences range from 10 to several hundred km/s as observed in the plane of the sky. For those features that rapidly evolve within the corona (CMEs), a mean event speed of 402 km/s was found from the examination of 1200 events observed by SMM between 1980 and 1989. Peak speeds detected in the plane of the sky are sometimes three times that value. At 400 km/s, CMEs in the plane of the sky have an angular velocity of about one solar radius per hour, a convenient number to keep in mind. Finally, the sound speed in the photosphere is 7 km/s and estimates of the Alfvén wave speed in the corona range from ~150 to 1000 km/s, depending on the assumed magnetic field strength.

With these time scales in mind, two images per day are probably satisfactory, but noisy, for determining the long-lived, large-scale coronal structures and their evolution. Transient events require more data. The general approach to picture taking and data handling is based on the concept that more science can be returned by lossy compression of an originally larger data base than by lossless compression of a smaller data base. Thus the instrument would take much more data than would be transmitted. One concept is to take a picture about every 6 minutes and to sample each picture over three annuli at different heights with 5° resolution and a data rate of ~1 bps. CMEs could be easily identified by such scans, which can be used as an on-board tool for managing the selection of data for transmission. Even the fastest CMEs, which would move through the field of view in ~3 hours, could be caught in 30 consecutive images. While this transient-detection scheme would require two 30-Mbit buffers, the average downlink rate could be reduced to $< \sim 1$ kbps.

Other requirements of the coronagraph are included in Table 4.6 at the end of this Section.

B. Disk Imager

This instrument is currently not well defined. It could take any of a number of forms, depending in the ingenuity of the instrument provider(s) and their success in the on-going development of low-mass instruments. The requirements provided as input to the technical feasibility study (Table 4.6) are really allocations, not to be exceeded. One requirement unique to this instrument is placed on the post-facto knowledge of the spacecraft orientation about the Sun-spacecraft line; one pixel of rotation for a 1024x1024 CCD translates into 0.1° roll knowledge.

Ideally, this instrument would serve as both a magnetograph (measuring the radial component of field would meet the major objectives) and a Dopplergraph to measure radial flow velocities. Sufficiently light-weight instruments do not currently exist, but development efforts are underway. Since mass is at a premium, it might make sense to combine the detector and electronics of the disk imager with that of the coronagraph.

Even much simpler instruments could be very valuable. For example, for a few kg, one could use multilayer filters and simple detectors in soft x-rays or the ultraviolet to distinguish patterns of open versus closed field lines. A useful wavelength for disk imaging would be the helium Lyman-alpha line at 304 Å. The Si XI line is useful for observing off-limb images of magnetic structures.

C. All-Sky Camera

The purpose of the All-Sky Camera (ASC) is to trace coronal features through interplanetary space. Analogous to coronagraphs, “all-sky” photometers detect solar radiation Thomson-scattered from free electrons in the interplanetary plasma. This technique was used by Jackson and Leinert (1985) to determine the brightness, number flux, temporal variations, speed, and spatial distribution of large-scale features propagating through the heliosphere. Those features include CMEs (Jackson 1985; Jackson et al., 1985; Webb and Jackson, 1990), coronal streamers (Jackson, 1991), interplanetary shock waves, and comets and cometary bow shocks. Using a single camera, it is possible to deconvolve the density of material within those structures using different views as the structure passes the spacecraft (see cover).

The strawman ASC is based on heritage from the photometer system on the Helios mission and from a second-generation instrument called the Solar Mass Ejection Imager (SMEI). SMEI is an all-sky viewing instrument currently funded by the Air Force and NASA to be built at Phillips Laboratory, at the University of Birmingham, England, and at the University of California at San Diego. It is expected to be ready for launch by the Air Force Space Test Program in the year 2000. Jackson et al. (1996) have recently documented the expected capabilities of the instrument.

The important parts of the ASC are a fish-eye lens (Smith, 1992), a CCD detector and a baffle system. The baffle is a corral-like enclosure with five concentric knife-edge walls, with each edge progressively obscuring the previous one. The outer diameter of the baffle

system is ~ 45 cm. The baffle reduces direct sunlight and reflections from illuminated portions of the spacecraft by a factor of 10^{-12} provided they are not within 90° of the normal to the instrument. A sketch of the baffle concept is shown in Figure 4.1 and a photo of a mechanical mockup is shown in Figure 4.2.

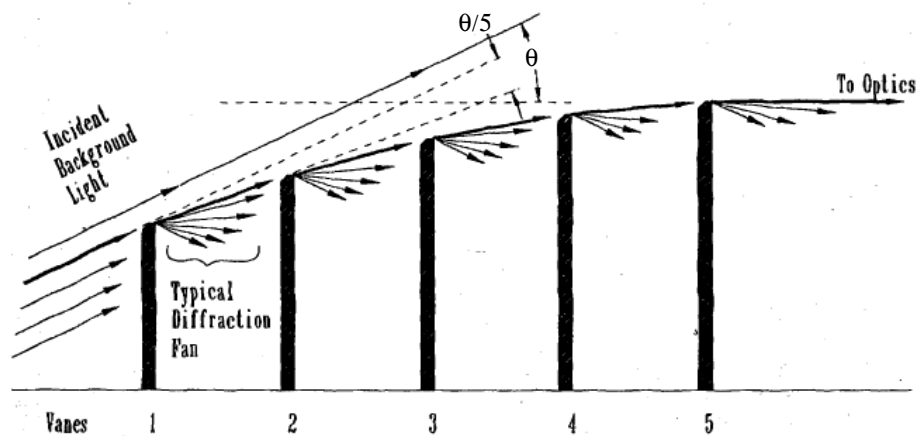


Figure 4.1. Schematic illustrating baffle concept. The background light diffracts off the sequence of vanes as shown by a fan of rays on each. Vane heights are chosen so each has a diffraction angle of θ/N for the ray just reaching the next vane edge. From Buffington et al. (1996).



Figure 4.2. Photo of mechanical mockup of an all-sky camera suitable for use on SPSM.

The photometer system is designed to detect changes in sky brightness at the level of ~ 1 S10 unit (the equivalent of a tenth magnitude star in one square degree of sky) at 90° elongation from the Sun-spacecraft line. Table 4.2 provides estimates of different heliospheric signals at various angular separations from the Sun. A photometric precision of 0.1% would allow relatively clean separation of heliospheric structures from the zodiacal

light and stellar background, although some heliospheric features will have sufficient brightness and contrast that 0.1% photometric precision is not necessary.

TABLE 4.2. REPRESENTATIVE SIGNAL LEVELS IN S10 UNITS AT SEVERAL SOLAR ELONGATION ANGLES AS SEEN BY A SPACECRAFT AT 0.48 AU.

Observed Phenomenon	Brightness @ 10°	Brightness @ 60°	Brightness @ 130°
Zodiacal light (ecliptic)	120,000	1500	640
Zodiacal light (latitude = 30°)	1400	760	500
Average star brightness	105	105	105
Coronal mass ejections	300-800	3-8	1-4
Streamer	140-400	1-4	0.4-2
Shock	140-400	1-4	0.4-2
Comet bow shock	40-200	n/a	n/a

A neutral density filter ($D \approx 1.0$) attenuates the field inside 20° elongation to allow a single unsaturated exposure to be obtained. The instrument is also equipped with a focus mechanism and a shutter which is sufficient to withstand direct sunlight when the spacecraft is offset from the Sun for telemetry sessions.

SPSM might carry two all-sky cameras, like a pair of ear muffs, one on each side of the spacecraft to enable imaging of almost the entire sky. The mass and power requirements would be 4 kg and 8 w. For the feasibility study described in the Section VII, however, it was assumed that there would be only a single ASC with a mass of 3 kg.

The basic product of the ASC is one picture an hour with $1^\circ \times 1^\circ$ resolution. Each picture can be built up from six consecutively-obtained pictures of a few tens of seconds exposure with the resolution allowed by a 4096×4096 CCD detector. Before the final image is created and compressed, the higher resolution data can be manipulated to remove cosmic-ray hits.

Although the ASC is designed for studying heliospheric structures, several other types of observations are also possible.

- The zodiacal cloud has never before been viewed from above the solar poles. The brightness of dust in space beyond the zodiacal cloud is unknown. Interstellar dust and its asymmetries, flow direction, and variability should be measurable from the perspectives provided by the SPSM trajectory.
- It is expected that a near-Earth instrument with the capabilities of the ASC would detect between 10 and 100 asteroids per year with radii ≥ 12 m. In a polar orbit at 0.48 AU, where the distribution and motions of asteroids are not known, the instrument would provide fundamental information about the spatial distributions, motions, and total numbers of these objects.
- Comet views from non-Earth perspectives are of interest in mapping the locations of various parts of comet gas and dust tails. Views of comets and the distribution of dust to the level of the zodiacal cloud brightness would provide fundamental information about the dust replenishment of the zodiacal cloud.

- Precise photometric times series can be obtained for the brightest stars.
- The ASC could be used to image the solar sail during cruise for some orientations of the sail.

D. Plasma Analyzer and Magnetometer

A rather simple package of plasma instruments is required to relate the properties of the solar wind at 0.48 AU to the solar and coronal features studied with the remote sensing instruments. In order to distinguish one type of solar wind stream from another and transient from quasi-stationary flow, the instrument package should contain (1) a vector magnetometer, (2) a solar-oriented ion analyzer capable of measuring the vector velocity, density, temperature, and anisotropy of protons and alpha particles, and (3) an electron detector with the fields of view required to determine the presence or absence of the counterstreaming superthermal (~ 100 eV) electrons diagnostic of CME-associated flow. It would also be highly desirable, if it can be accommodated within the mass allocation, to obtain some measure of heavier, trace ions. A particularly important plasma diagnostic would be the distribution of charge states of oxygen ions.

The ion measurements should cover the range 250 eV/q to ~ 50 keV/q, while the electron measurements should cover the range 2.5 eV to 50 keV. The top end of that range, from 1-50 keV, was not sampled by Ulysses and may be important for understanding ion-acoustic-like electrostatic instabilities and control of the electron heat flux in the solar wind. A time resolution of ~ 5 minutes per spectrum is adequate to meet the objectives. The data can be strongly compressed; for example, ion measurements in the form of a bi-kappa distribution for protons and alphas would require only 18 parameters per spectrum, or 36 parameters per spectrum if one allowed for double beaming.

There is a special challenge in measuring the vector velocity and the three dimensional plasma distribution functions from a 3-axis attitude-stabilized spacecraft such as SPSM. Either of two approaches used in the past should prove to be adequate, however. The first is a Faraday cup with segmented collectors to allow determination of directions, while the second is a spherical section electrostatic analyzer with electrostatic deflection to obtain information in the third dimension.

The magnetometer must be capable of measuring the vector magnetic field; either a fluxgate or a helium magnetometer would suffice for the relatively strong fields to be encountered at 0.48 AU. The spacecraft field must be low (preferably < 1 nT), known, and constant so the magnetometer data can be corrected on-board and then used in reducing the plasma distributions from the three-dimensional measured distributions to the two-dimensional, field-aligned distributions to be telemetered. The use of a 1-m boom was assumed for the technical feasibility study.

E. Energetic Particle Telescopes

The energetic particle objectives of SPSM require instrumentation capable of a) identifying both gradual and impulsive solar energetic particle (SEP) events by their composition and

other characteristics; b) identifying interplanetary particles accelerated by traveling and co-rotating interplanetary shocks; c) measuring the spectra of the dominant elements that comprise the anomalous cosmic ray (ACR) component (e.g., He, N, O, and Ne); and 4) measuring low-energy (<100 MeV/nucleon) spectra of the dominant species in the galactic cosmic ray (GCR) component (e.g., H, He, C, O, Ne, Mg, Si, and Fe). These measurements should span as large a dynamic range as possible (e.g., 0.1 to -100 MeV/nucleon), consistent with the available resources.

Gradual and impulsive SEP events can be identified by their temporal behavior and distinguishing compositional characteristics (see Table 4.3), which requires measurement of electrons, ^3He , and elemental composition up through the Fe-group. Interplanetary and co-rotating shock events can be distinguished by correlating the particle measurements with plasma and field data. Their energy spectra are typically softer than in SEP events and are best studied at energies of ~1 MeV and below. The objectives pertaining to anomalous and galactic cosmic rays can be met by measurements in the energy range from ~3 to 50 MeV/nucleon. None of the objectives requires isotopic resolution except for the need to identify ^3He -rich impulsive flares. Table 4.4 summarizes measurement objectives that meet these requirements. If additional resources are available it would clearly be desirable to extend the energy ranges of some of these species, and/or to increase the collecting power of the sensors.

TABLE 4.3. OBSERVATIONAL CHARACTERISTICS THAT CAN BE USED TO DISTINGUISH BETWEEN IMPULSIVE AND GRADUAL SEP EVENTS.

Impulsive Events

Enriched in ^3He
 Electron rich
 Enriched in Fe & other heavy ions
 Rapid rise & decay

Gradual Events

Normal isotopic composition
 Proton rich
 Coronal abundances
 More Extended

TABLE 4.4. MINIMUM MEASUREMENT OBJECTIVES FOR ENERGETIC PARTICLES

Electrons:	~0.1 to 5 MeV
Protons:	~0.1 to 50 MeV
Helium:	~1 to 50 MeV/nucleon
Heavy Elements:	~3 to 50 MeV/nucleon
^3He identification	
On-board processing of data to identify composition characteristics and energy spectra.	

Meeting these objectives with instrumentation that requires the minimum resources (especially mass) requires several particle telescopes. Three complementary sensors can accomplish this; they are labeled SEP, LET, and HET. They are all based on silicon solid state detectors, and draw heavily on previously flown designs that have proven successful

in earlier interplanetary missions.

The Solar Electron & Proton (SEP) sensor system, illustrated in Figure 4.3, consists of two nearly identical telescopes. A 330 microgram/cm² foil on one telescope allows 30 keV to 0.7 MeV electrons and 50 keV to 6 MeV protons to be separately identified by a differencing scheme. The system is based on a design developed by GSFC that was to have flown on the US spacecraft for the International Solar Polar Mission (now known as Ulysses). It is especially suited to studying impulsive events at low energy.

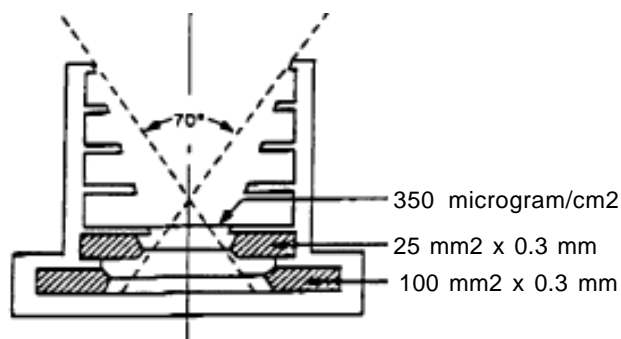


Figure 4.3 Diagram of the Solar-Electron-Proton telescope

The Low-Energy Telescope (LET) shown in Figure 4.4 is based on a design flown on Voyager. It can identify elements from H to Ni in the energy range from ~3 to 50 MeV/nucleon, and can also separate ³He from ⁴He.

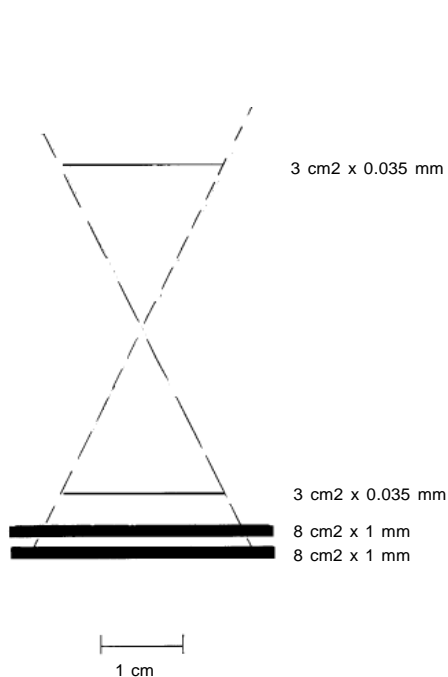


Figure 4.4 Low-energy telescope concept

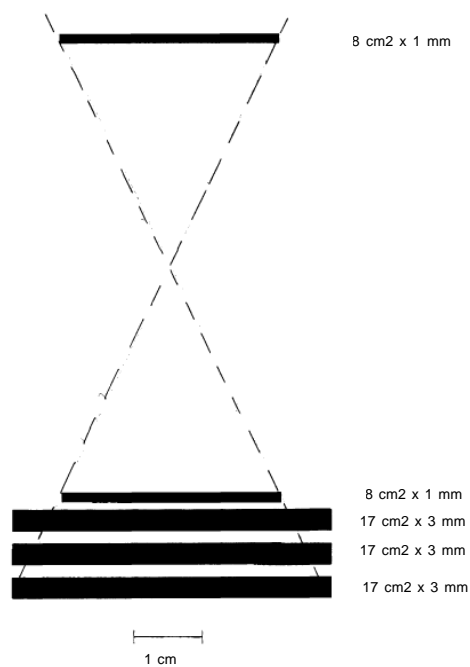


Figure 4.5. High-energy telescope concept

The High Energy Telescope (HET) shown in Figure 4.5 is a simple system that extends the measurements of protons, electrons, and heavier elements to higher energies. The thickness of the telescope is defined by the need to measure high energy H and He, and in solar particle events it will extend the energy spectra of protons and helium to energies of ~80 MeV/nucleon. During quiet times it will measure the ACR and GCR spectra of nuclei up through the Fe-group to energies of several hundred MeV/nucleon.

The energy ranges covered by these sensors are summarized in Table 4.5; note that they meet all of the measurement objectives in Tables 4.3 & 4.4.

TABLE 4.5. ENERGY RANGES FOR STOPPING PARTICLES (MEV OR MEV/NUC)

<u>Species</u>	<u>SEP</u>	<u>LET</u>	<u>HET</u>	<u>HET Penetrating</u>
Electrons	0.03 to 0.7	-	1 to 6	>6
Protons	0.05 to 6	2 to 13	13 to 41	41 to ~80, >80
Helium	>1.5	2 to 13	13 to 41	41 to ~80, >80
Oxygen		3.5 to 29	28 to 90	90 to ~180, >180
Iron		4 to 48	47 to 170	170 to 340, >340

Note: "Penetrating" particles traverse the entire telescope. Abundant species can be identified by their energy loss over a limited energy range

These three telescopes together require ~1.5 kg and ~0.9 w. All of the detectors in the LET and HET telescopes could be individually pulse-height analyzed by custom low-power VLSI circuitry developed for the ACE mission. This circuitry provides 12-bit accuracy for ~40 mw per chain. The mass and power estimates are based on the assumption of a central data processing unit (DPU) and a central power system that provides the needed low voltages. For the feasibility study discussed in Section VII, it was assumed, however, that the resources for the energetic particle package are 2 kg and 1.5 w in order to include a DPU to compress the data from several hundred bps to ~30 bps. This compression is achieved by combining the energy-loss and total energy data to calculate the particle mass on-board.

SPSM will be a three-axis stabilized spacecraft that is pointed toward the Sun most of the time. Although it would clearly be desirable to have multiple telescopes pointed in several directions to allow for anisotropy studies, this is not required to meet the energetic-particle objectives, and is not possible if the mass of the payload is tightly constrained. The preferred orientation for all telescopes is in the general direction of the Sun in order to be most sensitive to SEP events. If additional resources become available it would be possible to mount additional telescopes looking in the anti-solar direction; to provide true 3-dimensional anisotropies requires a minimum of four telescopes, preferably looking in orthogonal directions, such as the LET system on Voyager. On the other hand, if the resources are even more tightly constrained, it would also be possible to combine the LET and HET telescopes into a single back-to-back telescope that still makes all of the same measurements for somewhat less weight and power. In this case the combined HET/LET system must be mounted so that both opposing fields of view are free of obstruction.

The solid state detectors in these telescopes should not be operated or stored at temperatures $>35^{\circ}\text{C}$.

F. Summary of Strawman Payload

Table 4.6 summarizes requirements of the strawman payload described above. These requirements served as input to the technical feasibility study described in Section VII. Some of the requirements are the results of iterations between the scientists' desires and the realities of mass and cost provided by the spacecraft engineers.

There are also several requirements that apply to the payload as a whole:

- The spacecraft should provide 10 Gbits of data storage to provide flexibility in the data return strategy.
- Data latency should normally be ≤ 1 week
- $\geq 90\%$ of the data transmitted data should be available and any corrupted data should be so identified.
- Once in the final orbit, the spacecraft should obtain data $\geq 90\%$ of the time.
- It is permissible to point the spacecraft off its nominal solar orientation during data transmission providing the requirement above is met.